GLOBAL BIOGEOCHEMICAL CYCLES, VOL. ???, XXXX, DOI:10.1029/,

Effects of anthropogenic land cover change on the carbon cycle of the last millennium

J. Pongratz,[1,2] C.H. Reick,[1] T. Raddatz,[1] and M. Claussen[1,3]

J. Pongratz, Max Planck Institute for Meteorology, Bundesstraße 53, 20146 Hamburg, Germany, and International Max Planck Research School on Earth System Modelling, Bundesstraße 53, 20146 Hamburg, Germany. (julia.pongratz@zmaw.de)

C.H. Reick, Max Planck Institute for Meteorology, Bundesstraße 53, 20146 Hamburg, Germany. (christian.reick@zmaw.de)

T. Raddatz, Max Planck Institute for Meteorology, Bundesstraße 53, 20146 Hamburg, Germany. (thomas.raddatz@zmaw.de)

M. Claussen, Max Planck Institute for Meteorology, Bundesstraße 53, 20146 Hamburg, Germany, and KlimaCampus, University of Hamburg, Hamburg, Germany. (martin.claussen@zmaw.de)

[1]Max Planck Institute for Meteorology,

Abstract. Transient simulations are performed over the entire last millennium with a general circulation model that couples the atmosphere, ocean, and the land surface with a closed carbon cycle. This setup applies a high-detail reconstruction of anthropogenic land cover change (ALCC) as the only forcing to the climate system with two goals: (1) to isolate the effects of ALCC on the carbon cycle and the climate independently of any other natural and anthropogenic disturbance and (2) to assess the importance of preindustrial human activities. With ALCC as only forcing, the terrestrial biosphere experiences a net loss of 96 Gt C over the last millennium, leading to an increase of atmospheric CO_2 by 20 ppm. The biosphere-atmosphere coupling thereby leads to a restorage of 37% and 48% of the primary emissions over the industrial (AD 1850–2000) and the preindustrial period (AD 800–1850), respectively. Due to the stronger coupling flux over the preindustrial period, only 21% of the 53 Gt C preindustrial emissions remain airborne. Despite the low airborne fraction, atmospheric CO_2 rises above natural variability

Hamburg, Germany.

[2]International Max Planck Research School on Earth System Modelling, Hamburg, Germany.

[3]KlimaCampus, University of Hamburg, Hamburg, Germany.

by late medieval times. This suggests that human influence on CO_2 began prior to industrialization. Global mean temperatures, however, are not significantly altered until the strong population growth in the industrial period. Furthermore, we investigate the effects of historic events such as epidemics and warfare on the carbon budget. We find that only long-lasting events such as the Mongol invasion lead to carbon sequestration. The reason for this limited carbon sequestration are indirect emissions from past ALCC that compensate carbon uptake in regrowing vegetation for several decades. Drops in ice core CO_2 are thus unlikely to be attributable to human action. Our results indicate that climate-carbon cycle studies for present and future centuries, which usually start from an equilibrium state around 1850, start from a significantly disturbed state of the carbon cycle.

1. Introduction

The vegetation covering the continents has a decisive influence on the climate. Through the uptake of CO_2 from the atmosphere, plants play a central role in the global carbon cycle. Furthermore, they influence the exchange of energy, water, and momentum between the atmosphere and the land surface. Humankind is altering these processes by transforming areas of natural vegetation to human use in agriculture, forestry, and urbanization ("anthropogenic land cover change", ALCC). The anthropogenic disturbance of the natural land cover has started thousands of years ago with the expansion of agriculture, and possibly earlier with hunters and gatherers managing woodlands for hunting and traveling. The disturbance has grown to create a human-dominated world today, as 30–50% of the Earth's land cover are substantially modified by human land use — primarily by the expansion of agriculture [Vitousek et al., 1997]. The recognition is growing that ALCC has an impact on climate and the carbon cycle and needs thorough investigation to understand its pathways of disturbance, its past and future effects, as well as its potential to mitigate climate change [Barker et al., 2007; Denman et al., 2007]. Consequently, land-use modules including carbon cycling are being developed for many terrestrial biosphere or climate models [e.g., McGuire et al., 2001; Strassmann et al., 2008]. They ideally calculate all fluxes endogenously and coupled to the atmosphere and ocean to allow for, e.g., a closed, interactive carbon cycle including biosphere-atmosphere feedbacks. Eventually, the recommendation was given to supply ALCC as spatially explicit information to the climate projections of the next report of the Intergovernmental Panel on Climate Change [Moss et al., 2008].

The influence of vegetation cover and ALCC on the climate is commonly divided into biogeophysical and biogeochemical mechanisms. The first include all modifications of the physical properties of the land surface such as albedo, roughness, and evapotranspiration. Modeling studies suggest that at mid- and high latitudes the increase of albedo is the dominant biogeophysical process of ALCC. Albedo increases as a consequence of deforestation — due to the higher snow-free albedo of non-forest vegetation as well as the snow masking effect of forest [Bonan et al., 1992] — and generally induces a cooling, possibly enforced by the sea ice-albedo feedback [e.g., Betts, 2001; Claussen et al., 2001; Bounoua et al., 2002]. In the tropics, the reduction of evapotranspiration following deforestation leads to a loss of evaporative cooling and counteracts the albedo effect. Tropical deforestation can thus lead to a local warming [e.g., Claussen et al., 2001; Bounoua et al., 2002; DeFries et al., 2002], although its effects on the extra-tropics may be a cooling from the reduced atmospheric content of water vapor acting as a greenhouse gas [e.g., Sitch et al., 2005].

Probably the most important biogeochemical mechanism of ALCC is the influence on the carbon cycle, and the associated impact on the global CO_2 concentration. Altering atmospheric CO_2, ALCC modifies the Earth's energy balance and thus climate. ALCC constitutes a source of emissions mainly from the loss of terrestrial biomass. About one third of the anthropogenic CO_2 emissions over the last 150 years are estimated to be the direct consequence of ALCC [Houghton, 2003a]. Counteracting the emissions is an increased carbon uptake by both natural and agricultural vegetation, the so-called "residual land sink" [Denman et al., 2007]. Through this effect, the biosphere mitigates anthropogenic greenhouse gas emissions. The causes of the land sink are not well specified and assumed to be, among others, the fertilizing effect of increased atmospheric CO_2, nitrogen deposition, recovery from past disturbances, and climate change [Schimel et al., 2001, and references therein]. The net effect is that the terrestrial biosphere has turned from a source to a sink during the recent decades. All these carbon fluxes, however, are very uncertain. The uncertainty range assigned to estimates of ALCC emissions is about $\pm 70\%$ even for the last — best-documented — decades, and propagates to the carbon sink term [Denman et al., 2007]. Difficulties in quantifying and locating ALCC are only one problem beside gaps in process understanding and model differences [McGuire et al., 2001]. Further complexity is added by the interaction of biogeophysical and biogeochemical effects and the two-way coupling of the carbon cycle and the climate.

Primary emissions by ALCC have first been estimated either by simple book-keeping approaches [Houghton et al., 1983] or by spatially explicit simulations of carbon stocks for different time slices by process-oriented models [DeFries et al., 1999; Olofsson and Hickler, 2008]. Primary emissions are now increasingly derived from transient studies, though only for the last three centuries. In these studies, carbon loss, uptake, and the net effect of ALCC on the carbon cycle are simulated. Climate and CO_2 fields may either be prescribed [McGuire et al., 2001; Jain and Yang, 2005], in which case no feedbacks from ALCC on the climate are allowed; or they may be calculated interactively. The latter method has been used for past and future ALCC in a range of studies applying Earth system models of intermediate complexity (EMICs) [Gitz and Ciais, 2003; Sitch et al., 2005; Brovkin et al., 2006; Strassmann et al., 2008]. Recently, second-order effects of ALCC were identified, such as the loss of carbon sink capacity by replacing forests with agricultural land [Gitz and Ciais, 2003]. Several studies have focused only on the net effect of potential ALCC scenarios and the resulting influence on climate of the biogeochemical effects in comparison to the biogeophysical ones [e.g., Claussen et al., 2001; Brovkin et al., 2004].

In the present study, we apply a general circulation model (GCM) for the atmosphere and the ocean coupled to a land surface scheme, considering both biogeophysical and biogeochemical effects of ALCC. Our model includes a closed carbon cycle (land, ocean, atmosphere) that evolves interactively with the climate. Feedbacks between the carbon cycle and the climate are thus included in the simulations. We distinguish between source and sink terms and identify further sub-processes of biosphere-atmosphere carbon exchange. A detailed reconstruction of ALCC is applied that indicates areas of cropland, pasture, and natural vegetation for each year since AD 800 [Pongratz et al., 2008], which allows us to quantify the effects of ALCC transiently over history. To our knowledge, the combination of method, data, and the length of the simulated time period makes this study the first to assess the effects of ALCC on the carbon cycle and the climate in such detail.

We do not try to simulate a realistic climate evolution as influenced by all natural and anthropogenic forcings, but we try to isolate the impact of ALCC on climate by allowing ALCC as the only forcing to the carbon cycle and climate system. Anthropogenic carbon emissions from fossil-fuel burning and cement production are the most important driver of CO_2 and climate change today, but did not grow significantly larger than ALCC emissions until the 1930s [Houghton, 2003a; Marland et al., 2008], and played no role in the preindustrial period. For the preindustrial era, our model results can therefore be expected to represent most of the real impact of human activity. The studies by DeFries et al. [1999]; Olofsson and Hickler [2008]; Ruddiman [2003, 2007] clearly indicate that significant amounts of carbon were already released in the preindustrial period, but estimates range from 48–320 Gt C. The net effect of preindustrial ALCC is even more disputed, ranging from a key climate forcing [Ruddiman, 2007] to a very small one [Joos et al., 2004]. It has also been suggested that historic events such as warfare and epidemics altered atmospheric CO_2 via their impact on agricultural extent [Ruddiman, 2007], but a thorough investigation has not been undertaken since, until recently, no spatially explicit information on the actual changes of vegetation distribution existed. Our study assesses the effects of historic events over the last millennium and gives new estimates for associated carbon source and sink terms. Including also the carbon cycle in the ocean, we can estimate the amount of carbon that remains in the atmosphere and address the question whether an anthropogenic influence on the carbon cycle, and finally climate, has existed prior to the industrialization.

2. Methods

2.1. Model

The atmosphere/ocean general circulation model (AOGCM) consists of ECHAM5 [Roeckner et al., 2003] at T31 (approximately 4°) resolution with 19 vertical levels representing the atmosphere, and MPI-OM [Marsland et al., 2003] at 3° resolution with 40 vertical levels representing the ocean. The two models are coupled daily without flux correction. The carbon cycle model comprises the ocean biogeochemistry model HAMOCC5 [Wetzel et al., 2005] and the modular land surface scheme JSBACH [Raddatz et al., 2007]. HAMOCC5 simulates inorganic carbon chemistry as well as phyto- and zooplankton dynamics in dependence of temperature, solar radiation, and nutrients. It also considers the buildup of detritus, its sinking, remineralization, and sedimentation. JSBACH distinguishes 12 plant functional types (PFTs), which differ with respect to their phenology, albedo, morphological and photosynthetic parameters. The fractional coverage of PFTs in each grid cell is prescribed from maps annually. For each PFT, the storage of organic carbon on land occurs in five pools: living tissue ("green"), woody material ("wood"), and a pool storing sugar and starches ("reserve") for the vegetation carbon, and two soil carbon pools with a fast (about 1.5 years) and a slow turnover rate (about 150 years). Three managed vegetation types are included in the 12 PFTs: cropland, with a specific phenology scheme, and C3 and C4 pasture, which are included in the two natural grassland types.

For this study ALCC was implemented in JSBACH as follows: The change in the cover fractions of PFTs (i.e. reduction of natural vegetation to cropland or pasture and reversion thereof, transition between cropland and pasture) is prescribed from the maps described below and linearly interpolated from annual changes to a daily timestep. With changes in the cover fractions, carbon is relocated between the pools. The vegetation carbon of PFTs with decreasing area is either directly released to the atmosphere, or relocated to the two soil pools. Carbon release directly to the atmosphere happens, e.g., when forest is cleared by fire, and a fraction of 50% of the vegetation carbon is chosen in this study as flux to the atmosphere. The choice of this value is not critical for the present analysis: The timescale of our study is multi-centennial and thus larger than the slowest turnover rate of the carbon pools, so that all vegetation carbon lost is eventually transferred to the atmosphere. The amount of ALCC carbon per m^2 and day directly released to the atmosphere from the three vegetation pools is calculated as

$$F_{\triangleright A} = \sum_{i \in a-} (c_i^{old} - c_i^{new}) \cdot (f_{G \triangleright A} C_{G,i} + f_{W \triangleright A} C_{W,i} + f_{R \triangleright A} C_{R,i}) \ , \qquad (1)$$

where $f_{G \triangleright A}$, $f_{W \triangleright A}$, and $f_{R \triangleright A}$ denote the fractions of carbon released to the atmosphere due to ALCC for the three vegetation carbon pools (green, wood, and reserve, respectively). $c_i^{old} - c_i^{new}$ denotes the daily change in cover fraction of the i-th PFT that loses area ($a-$) due to ALCC, and $C_{G,i}$, $C_{W,i}$, and $C_{R,i}$ denote the carbon densities of the three vegetation pools. For the relocation of vegetation carbon to the two soil pools, the carbon from the green and reserve pools is transferred to the fast soil pool in each grid cell, while the carbon from the wood pool is transferred to the slow soil pool. The long decay time of the slow soil pool implicitly includes the storage of carbon in long-term human use. The ALCC carbon fluxes to the fast and slow pool are calculated as

$$F_{\triangleright F} = \sum_{i \in a-} (c_i^{old} - c_i^{new}) \cdot [(1 - f_{G \triangleright A}) C_{G,i} + (1 - f_{R \triangleright A}) C_{R,i}] \qquad (2)$$

$$F_{\triangleright S} = \sum_{i \in a-} (c_i^{old} - c_i^{new}) (1 - f_{W \triangleright A}) C_{W,i} \ . \qquad (3)$$

Vegetation carbon is therefore lost from a PFT only due to the decrease of its area, while its carbon densities are unaffected. The carbon lost is then transferred to the respective soil carbon pools of the expanding PFTs, distributed proportionally to their new cover fractions, and the PFT carbon densities adjusted accordingly. This scheme describes the temporal evolution of land carbon storage for agricultural expansion as well as abandonment consistently.

2.2. ALCC data

As ALCC forcing, the reconstruction of global agricultural areas and land cover by Pongratz et al. [2008] is applied. It contains fractional maps of 14 vegetation types at an annual timestep and a spatial resolution of 0.5°. The agricultural types considered are cropland, C3, and C4 pasture. The reconstruction merges published maps of agriculture from AD 1700 to 1992 and a population-based approach to quantify agriculture for each country for the time period AD 800 to 1700. With this approach the general expansion of agriculture is captured as well as specific historic events, such as epidemics and wars, that are likely to have caused abandonment of agricultural area in certain regions due to their impact on population numbers. The uncertainty associated with the chosen approach, with respect to the uncertainty of population data and of agrotechnological development, was assessed in two additional datasets for AD 800 to 1700, which indicate the upper and lower range of possible agricultural extent.

A map of potential vegetation with 11 natural PFTs was used as background to the agricultural reconstruction with different allocation rules for cropland and pasture. Most previous studies that included pasture interpreted the expansion of pasture as deforestation or reduced all natural vegetation equally, not taking into account that in history humans used natural grasslands for pastures rather than clearing forested area [e.g., Houghton, 1999], thus overestimating ALCC. The ALCC reconstruction applied here implemented the preferential allocation of pasture on natural grasslands. An extension of the agricultural and land cover maps into the future follows the A1B scenario [Nakicenovic et al., 2000], superimposing changes in agricultural extent from the scenario maps on the map of 1992, the last map available from the ALCC reconstruction. Though not main focus of this study, the future period is included for a clearer depiction of the effects of ALCC.

ALCC other than caused by the change in agricultural extent, e.g., shifting cultivation and wood harvest on areas that are not subsequently used for agriculture, is not taken into account in this study. However, forestry for wood production is expected to have only a small effect on the net carbon balance, as harvest in most cases tends to be compensated by regrowth [Houghton, 2003a]. The same effect makes the distinction of agricultural area as either permanent or part of a system of shifting cultivation less important. Depending on the assumptions made concerning extent of the area under shifting cultivation and length of the fallow period, non-permanent agriculture may locally cause substantial emissions [Olofsson and Hickler, 2008]. In the present study, however, primary emissions are defined as the net carbon flux from the processes clearing and regrowth for each grid cell; considering the large size of each grid cell, the two processes largely cancel each other in particular with the long fallow period that is assumed for the preindustrial era [Olofsson and Hickler, 2008]. Soil carbon losses are further smaller than in the case of permanent agriculture [Houghton and Goodale, 2004]. For these reasons and due to the large uncertainties associated with determining extent and rotational cycle of shifting cultivation [Houghton and Goodale, 2004] we treat all agriculture as permanent in this study.

2.3. Simulation protocol

The model is spun up for more than 4000 years under CH_4, N_2O, solar, orbital, and land cover conditions of the year AD 800 until the carbon pools are in equilibrium. The final atmospheric CO_2 concentration is 281 ppm. Three simulations branch off from this equilibrium (Tab. 1): A 1300-year-long control simulation (named *ctrl*) keeps all forcings constant at the year AD 800 state, while two transient simulations run until the year 2100 applying ALCC as the only forcing (*LC*). The first applies the middle-range (*best-guess*) ALCC reconstruction with the aim to capture the impact of ALCC realistically; the second applies the lower-range ALCC reconstruction (*high land cover dynamics*, since it assumes less agricultural area in AD 800, but the same as the middle-range scenario after AD 1700) with the aim to give an upper limit of possible ALCC emissions and impact on climate and the carbon cycle for the preindustrial period. The transient runs simulate both biogeochemical and biogeophysical effects of ALCC and all atmosphere-ocean-biosphere feedbacks. They deliberately neglect natural and anthropogenic forcings other than ALCC, such as changes in the orbit, in the volcanic and solar activity, and the emissions from fossil-fuel burning. With this setup, it is thus possible to isolate the effect of ALCC on the climate and the carbon cycle.

In addition to the coupled simulations described above, the land carbon pools are re-calculated offline with the aim to separate the primary effect of ALCC on the carbon balance, i.e. prior to any feedbacks arising from the coupling with the climate and the atmospheric and marine part of the carbon cycle. In offline simulations any land cover history can be combined with any climate description. Derived from a coupled simulation, climate enters the offline simulation in the form of net primary productivity (NPP), leaf area index (LAI), soil moisture, and soil temperature and thus also includes physiological as well as climatic effects of changes in atmospheric CO_2. Two offline simulations are performed: In simulation L, the effects of ALCC were re-calculated under the climate of the control simulation. $ctrl - L$ then isolates the primary emissions of ALCC prior to any feedbacks (as positive flux to the atmosphere). The loss of carbon due to ALCC which is determined in this way, the "primary emissions", is directly comparable to book-keeping approaches such as by Houghton et al. [1983], which neglect any interactions between climate, CO_2, and the terrestrial carbon pools. $L - LC$, on the other hand, isolates the coupling flux, i.e. the influence that climate and CO_2 exert on carbon uptake and release by the biosphere. In the second offline simulation, C, the carbon pools are re-calculated for constant land cover of the year AD 800 under the climate and CO_2 from the coupled transient simulation. The difference between $L-LC$ and $ctrl-L$ quantifies the difference of primary emissions created under changing climate as compared to those created under the stable control climate.

Simulation results are often summarized in the following for the preindustrial (AD 800–1850), industrial (1850–2000), and future (2000–2100) period. The choice of the end date of the preindustrial era is based on the evolution of emissions from fossil-fuel burning. Cumulative fossil-fuel emissions are estimated at below 1.5 Gt C before AD 1850 [Marland et al., 2008] and have therefore negligible effects on the carbon cycle.

3. Primary emissions and terrestrial carbon cycle feedback

3.1. Overview

With ALCC as only forcing, the land biosphere remains a net source of carbon throughout the last millennium (Fig. 1). It loses 96 Gt C between AD 800 and 2000 (see Tab. 2 for the preindustrial, industrial, and future period). This results from a loss of vegetation carbon only partly offset by a gain in soil carbon, similar as in previous studies [e.g., Jain and Yang, 2005] (Fig. 2, $LC - ctrl$). Primary emissions are significantly higher than the net emissions, with 161 Gt C. The difference of 65 Gt C is the consequence of the coupling flux: The primary emissions alter climate and increase atmospheric CO_2 concentration (see Sec. 4.1). These changes enhance carbon uptake by the biosphere, in particular via CO_2 fertilization. As a consequence, 40% of the primary emissions over the last millennium are buffered by the biosphere.

3.2. Spatial patterns

The spatial distribution of the primary emissions, the coupling flux and the net emissions are shown separately for the preindustrial, the industrial, and the future period in Fig. 3. The maps for the net emissions contrast clearly the regions where agricultural expansion was strong during the respective time period and emissions are higher than the terrestrial sink, and those regions where carbon uptake from the coupling flux is stronger, usually the remaining pristine regions. In the preindustrial period, emissions arise primarily from Europe, India, China, and, in the last preindustrial centuries, North America, while a shift into tropical regions can be observed for the industrial times. Some regions show similar emissions for preindustrial and industrial times, but it needs to be kept in mind that the time span is very different (1050 vs. 150 years). The future scenario is characterized by reforestation in the midlatitudes and further emissions from the tropics. The strength of loss per converted area depends mainly on the biomass density. Negative emissions arise in some regions, where in the model cropland is more productive than the natural vegetation. The coupling flux shows an uptake of carbon in most areas, especially in the tropics. Only in few regions a carbon loss is simulated, which is probably a result from a climate change that is unfavorable for the prevailing vegetation. Apart from these areas, the change in CO_2, not a change in climate, seems to be the key factor for carbon uptake. The dominance of CO_2 fertilization for terrestrial carbon uptake cannot be proven with the present setup, but has been shown by previous studies [e.g., Jain and Yang, 2005; Raddatz et al., 2007] and is also suggested here, since the relative increase in NPP is homogeneous over all latitudes (not shown) and the climate signal is weak, especially in preindustrial times (see Sec. 4.2).

3.3. Primary emissions

Our quantification of the primary emissions for the preindustrial and industrial period is compared to previous studies in Tab. 3. We simulate primary emissions of 53 Gt C for the years AD 800 to 1850; approximately 10 Gt C must be added to take into account the emissions prior to AD 800 (assuming that the same amount of carbon is emitted per m^2 of agricultural expansion prior to 800 as averaged for 800 to 1850). Our estimates thus fall within the range given by DeFries et al. [1999] and Olofsson and Hickler [2008]. The values by Olofsson and Hickler [2008] may overestimate emissions since they implemented agricultural expansion entirely as deforestation. Our estimates are lower than the ones by Ruddiman [2003, 2007], who, however, takes into account several additional emission processes including some unrelated to ALCC, such as coal burning in China. The uncertainty estimate from the simulation with high land cover dynamics indicates that our primary emissions may be up to 8 Gt C or 15% higher over preindustrial times, which would also lead to a larger net carbon loss (Fig. 1). For the industrial period, we simulate primary emissions of 108 Gt C. This value is similar to other studies, though at the lower end, because most studies include additional processes such as wood harvest and shifting cultivation (Olofsson and Hickler [2008] include non-permanent agriculture in their high estimate, and DeFries et al. [1999] uses Houghton [1999] for the industrial value, including thus wood harvest).

The primary emissions are composed of two parts (Fig. 1): (a) A direct, instantaneous release of carbon to the atmosphere from the vegetation biomass during the process of conversion (accounting for 94 of the 161 Gt C emissions from AD 800 to 2000). This implicitly includes respiration of plant products in short-term human use, e.g. as domestic fuel. (b) Indirect emissions from the decrease in net ecosystem productivity (NEP; defined as NPP$-$R$_h$, where R$_h$ is heterotrophic respiration) (67 of the 161 Gt C). This implicitly includes respiration of plant products in long-term human use, e.g. as construction wood. NEP decreases since the decrease of NPP — the result of the ALCC-related change in area of differently productive PFTs — is not entirely balanced by a decrease of R$_h$. R$_h$ decreases less than expected for the equilibrium state due to (1) additional plant material added to the soil pools from the converted natural vegetation and (2) excess soil organic matter from past conversions, which accumulates due to the time lag of R$_h$ to NPP. The disequilibrium between NPP and R$_h$ is depicted in Fig. 4: Fig. 4a shows the changes in the transient coupled simulation, where both NPP and R$_h$ increase, but no apparent disequilibrium occurs. The change in land cover alone, however, decreases NPP stronger than R$_h$ (Fig. 4b) due to the additional and excess soil organic matter. The disequilibrium vanishes in the future afforestation scenario. The coupled simulation seems to be in balance because the disequilibrium with respect to primary emissions is balanced by a disequilibrium with respect to the coupling flux: with altered climate and increased CO_2 but unchanged land cover, NPP increases stronger than R$_h$ due to the time lag of R$_h$ to NPP (Fig. 4c). The latter disequilibrium has been called an “intriguing possibility” by Denman et al. [2007] in the context of a tropical forest sink.

The indirect emissions lead to an increase of soil carbon in the long term (Fig. 2), though this only slightly compensates the loss of vegetation carbon. This increase of soil carbon seems in disagreement with observational studies [see the meta analyses by Guo and Gifford, 2002; Murty et al., 2002]; these find that the transformation of forest to cropland is associated with a loss of soil carbon by, on average, 30% to 42%, while deforestation for pasture generally leads to a small gain. Indeed, many of the processes reducing soil carbon are not captured by our biosphere model, such as harvest losses, deprotection and erosion of soil organic matter under management. However, on the global scale, the modelled evolution of soil carbon stocks may still capture the realistic trend: The observational data generally refers to measurements at single points conducted 10 or more years after the land cover change. It therefore does not capture that simultaneously plant material has been added to the soil pools in regions of recent land cover change, at an increasing rate over history. Furthermore, much of the eroded material is likely to be replaced from cultivated fields to adjacent areas rather than being lost from the soil carbon stocks to the atmosphere and ocean. The increased transfer of plant material to the soil pools, especially of woody parts with slow decomposition rates, leads to "committed" future carbon emissions beyond the instantaneous ALCC. This committed flux becomes the dominant source of emissions in the afforestation scenario of the future (Tab. 2).

3.4. Coupling flux

The quantitative estimates of the coupling flux in this study cannot be compared directly to previous studies, as those include changes in CO_2 from fossil-fuel burning in addition to ALCC emissions. While those studies assume that present CO_2 lies 70–100 ppm over the preindustrial level, CO_2 in our study rises only by 20 ppm (thus close to the 18 ppm found by Brovkin et al. [2004] in a comparable EMIC study). In particular due to lower CO_2 fertilization the coupling flux in our study is thus lower than found e.g. by Gitz and Ciais [2003]; Denman et al. [2007]. As described before, the coupling flux leads to carbon uptake because of an increasing disequilibrium between NPP and heterotrophic respiration (Fig. 4c). The absorbed carbon is primarily stored in the soil carbon pools (Fig. 2). The larger amount of carbon stored in soils than in vegetation reflects the proportion of soil and vegetation pools and is the expected response to a comparatively small forcing over a long timescale.

The coupling flux increases NEP stronger, though only marginally, than has been determined above as overall strength of the coupling flux from the difference in total terrestrial carbon. The small counteracting effect is the coupling effect on the direct emissions: with the coupling to the altered climate and increased CO_2, more carbon is stored in the vegetation than would be under the control climate and unaltered CO_2 — and more carbon is thus released in the conversion of vegetation with ALCC. This effect amounts to only 2 Gt C until 2000.

Gitz and Ciais [2003] were the first to quantify the "land-use amplifier effect" ("replaced sinks/sources" in Strassmann et al. [2008]). This denotes the effect that ALCC "acts to diminish the sink capacity of the terrestrial biosphere by decreasing the residence time of carbon when croplands have replaced forests". In other words, the additional biosphere sink that arises under rising CO_2 is not as large as would be under natural vegetation, because storage in woody biomass ceases (carbon turnover rates are thus higher for cropland). Gitz and Ciais [2003] estimate that this effect may be as high as 125 Gt C over the 21st century for the A2 scenario. Calculation of the land-use amplifier effect in our study that most closely imitates their setup is to determine the loss of NEP for $C - LC$. For ALCC over the industrial period, this yields 49 Gt C. This cumulative flux, however, is composed of two parts: Only one part is the actual loss in additional sink from increased turnover rates that is intended to be quantified. The other part are indirect emissions from past ALCC. By comparing one simulation with static to one with transient land cover, both under changing CO_2 and climate, Gitz and Ciais [2003] implicitly include in the land-use amplifier effect the indirect emissions. In our simulation, indirect emissions amount to 45 Gt C, derived from the changes in NEP for $ctrl - L$ (Tab. 2). The indirect emissions have to be subtracted from the 49 Gt C in order to isolate the loss of additional sink capacity, which then amounts to only 4 Gt C. The relative difference between indirect emissions and loss of sink capacity is certainly not as high in the setup by Gitz and Ciais [2003] as here, since their study has a stronger increase of CO_2 by also including fossil-fuel burning, and the underlying ALCC is different. Still, with its analysis of sub-fluxes, our study suggests that a substantial fraction of the land-use amplifier effect results from the indirect emissions and thus from past ALCC, rather than from the change in current turnover rates.

4. Anthropogenic influence on the preindustrial carbon cycle and climate

During the preindustrial period, a lower fraction of the emissions remains in the atmosphere than during the industrial period (Tab. 4): biospheric uptake amounts to 48% of the emissions over the preindustrial period, as compared to only 37% for the industrial, fossil-fuel-free, period in this study. The difference to the industrial period is even greater when a realistic industrial period is considered that includes fossil-fuel burning: then, only 24–34% of the emissions are taken up by the biosphere, because of the additional emissions from fossil-fuel combustion (Tab. 4). This difference in strength of biospheric uptake between the industrial and preindustrial period is mostly the result of a stronger coupling flux in the latter. The slow and more linear increase of emissions gives the land biosphere more time for CO_2 uptake, and CO_2 fertilization is more efficient at low CO_2 concentrations. The relative uptake by the ocean is almost unaffected and remains at around one third.

4.1. Anthropogenic contribution to Holocene CO_2 increase

As a consequence of the strong buffering of primary emissions by the biosphere and the low airborne fraction of CO_2 in the preindustrial period, the simulations show an only slow increase of atmospheric carbon content, despite significantly altered carbon pools of the ocean and the land biosphere several centuries earlier already (Fig. 5). Atmospheric carbon increases by 11.5 or 13.4 Gt C over the time period 800 to 1850 (5 or 6 ppm) for the best-guess ALCC and high land cover dynamics, respectively. When we assume the same airborne fraction prior to AD 800 as for 800 to 1850 and calculate the change in atmospheric carbon proportionally to agricultural expansion, ALCC prior to 800 would add roughly 2.1 or 1.1 Gt C (1 or 0.5 ppm, best-guess ALCC and high land cover dynamics, respectively). If we accounted fully for the net emissions prior to AD 800, atmospheric CO_2 may have risen above natural variability prior to AD 800 already. However, especially the ocean uptake must be expected to have been even more efficient in the early period of the Holocene, both because uptake by dissolution is higher with lower CO_2 release and because carbonate compensation gets effective at the millennial timescale [Archer et al., 1997]. It seems thus plausible to neglect these small early net emissions. In this case, atmospheric carbon content has not increased beyond natural variability until the late medieval times, when net emissions grew larger than the natural variability in land-atmosphere CO_2 exchange (see Fig. 5). This happens rather independently of the ALCC scenario, since the largest differences between the scenarios occur only later with stronger population growth in the 16th and 17th century.

With an increase of atmospheric CO_2 by 5–6 ppm by AD 1850, our estimates of the anthropogenic contribution to the Holocene rise in CO_2 are similar to the ones by Ruddiman [Ruddiman, 2003, 2007]. Ruddiman suggests in his "early anthropogenic hypothesis" that preindustrial ALCC emissions increase CO_2 by at least 9 ppm — of which about half are resulting from ALCC — and are responsible, via several feedbacks, for the anomalous CO_2 increase during the Holocene of 40 ppm. A discrepancy arises, however, when one considers that much of the anomaly in Ruddiman's study has been built up already in the early preindustrial period, while less than half of the net emissions indicated above for AD 800 to 1850 in our study occur before 1700. This discrepancy may be explained by the difference in method and data: Ruddiman derives his estimates by assuming one global terrestrial carbon stock and one global value for the per-capita use of agricultural areas, which is simplified in comparison to the present study that applies a spatially and temporally detailed reconstruction of ALCC and that explicitly models terrestrial carbon coupled to the atmosphere and ocean. Especially the coupling of the biosphere to atmospheric CO_2 and to the ocean seems to be a major improvement, since it proofs to be the reason why preindustrial primary emissions become effective only to the small part of 21%. The present study further cannot support Ruddiman's hypothesis that the ALCC-induced release of CO_2 increased temperatures which in turn triggered an outgassing from the ocean. In our study, surface temperatures do not rise significantly in preindustrial times (Sec. 4.2) and the ocean remains a carbon sink throughout the last millennium. Since the present study indicates a substantially smaller anthropogenic influence on the global carbon cycle than the early anthropogenic hypothesis, it supports studies that suggested additional reasons like temporally limited post-glacial vegetation regrowth and carbonate compensation to explain the CO_2 anomalies (see, e.g., Claussen et al. [2005] for a discussion).

4.2. Effect of ALCC on global mean temperatures

A significant impact of ALCC on global mean surface temperature does not occur until the industrial period, when temperature starts to rise beyond the natural variability (Fig. 6). Changes are small not only because of the low airborne fraction of CO_2 and thus small greenhouse effect, but also because biogeophysical and biogeochemical effects are counteracting each other. The anthropogenic influence on global mean temperature thus begins even later than on atmospheric CO_2.

4.3. Epidemics and warfare

In addition to the hypothesis of CO_2 rising anomalously during the Holocene, Ruddiman [2007] also suggests that 1–2 ppm of several sudden CO_2 drops of up to 8 ppm, which are reconstructed from ice core records, can be explained by epidemics. Epidemics as well as warfare have the potential to change land cover since natural vegetation regrows on those agricultural areas that have been abandoned in the course of the many deaths. Through this, previously released CO_2 could again be sequestered. The land cover reconstruction applied in this study indicates, for example, a forest regrowth on about 0.18 million km^2

as a consequence of the Black Death, which arrived in Europe in 1347 and killed about one third of the population [McEvedy and Jones, 1978]. Other such historic events during the last millennium are the conquest of Middle and South America by the Europeans and both the Mongol invasion in China and the upheavals after the fall of the Ming Dynasty.

Although the conquest of Middle and South America led to a mass mortality by epidemics as well as direct warfare (the ALCC reconstruction used in this study assumes that 66% of the 40 million people died), this event does not imply large areas of regrowing vegetation and alters global carbon fluxes only negligibly. With total cumulative emissions of below 0.3 Gt C AD 800 to 1500 this region contributes only 2% to global emissions; even a sequestration of the entire 0.3 Gt C would be compensated by global emissions within 6 years and could therefore not be detected in ice core records. The reason for the few regrowing areas is mainly the assumption of a low per-capita use of agricultural land by the native Americans, but uncertainties are high in this region; for details see Pongratz et al. [2008]. Regrowth happens on larger areas, however, during the epidemics and warfare in Europe and China.

As explained in Sec. 3.3, ALCC does not only imply instantaneous, but also indirect future emissions from changes in NEP, which arise due to the imbalance of the soil carbon pools after ALCC. The strength of the indirect emissions of past ALCC as compared to the carbon sequestered in regrowing vegetation determines whether farm abandonment turns a region into a carbon sink or not; transient simulations are essential to capture this process. The Black Death and the 17th century upheavals in China, for example, bring emissions from NEP changes to zero or close to it, but do not lead to negative emissions, i.e. carbon uptake from regrowth (Fig. 7). The amount of carbon sequestered in the regrowing vegetation is thus balanced by the indirect emissions. For the Mongol invasion, on the other hand, NEP increases after two decades and leads to an overall carbon sink. We must thus distinguish two kinds of events: In weak events indirect emissions from past ALCC keep a region as carbon source despite declining agricultural area, while in strong, long-lasting events the increase of NEP with vegetation regrowth turns a region into a carbon sink. In all events, direct emissions vanish of course during the time of agricultural decline.

Even if a region becomes a carbon sink, the global impact of such historic events remains small: even during the Mongol invasion the global emission rates decrease, but do not get negative (Fig. 7). Other areas in the world with unperturbed agricultural expansion outdo the regional carbon uptake. This is valid, according to our simulations, even if we take into account the uncertainty of relevant parameters such as turnover rates of soil carbon: If we assume as a maximum estimate of carbon uptake that the entire area returns to its state of AD 800 within 100 years (the approximate time of tree maturing) after the epidemic or war, global emissions over the following 100 years always compensate the maximum regional regrowth. From this study, it thus seems implausible that regrowth on abandoned agricultural areas following epidemics and warfare, as suggested by Ruddiman [2007], caused the CO_2 drops reconstructed from ice core data. Not taken into account so far, however, is the global coupling flux, which restores almost half of the primary emissions (Sec. 4). It amounts to about 12 Mt C per year averaged over 800 to 1500, and 48 Mt C per year 1500 to 1700. These values are close to the respective minima in global primary emissions, so that global carbon sequestration may indeed temporarily occur. The coupling flux is, however, highly variable even on a centennial timescale, imposing a high variability also on the atmospheric response, as seen in Fig. 5c. Drops in CO_2 of several ppm may thus indeed occur, but can entirely be explained by natural variability.

5. Conclusions

For the first time, transient simulations are performed over the entire last millennium that apply a general circulation model with closed marine and terrestrial carbon cycle. With this setup we quantify the effects of ALCC on the carbon cycle and climate isolated from other natural and anthropogenic forcings. For the preindustrial period, the magnitude of the simulated carbon fluxes can be expected to reflect these fluxes realistically, since ALCC is the only anthropogenic forcing and the only major natural forcing — volcanoes — acts on a short timescale only. For the industrial period, the simulated results for both climate and the carbon cycle are significantly different from observations. By neglecting the emissions from fossil-fuel burning, the increase of atmospheric CO_2 is smaller than observed, with consequences on the strength of feedbacks, e.g., lower CO_2 fertilization.

Results show that without additional CO_2 fertilization from fossil-fuel burning, the biosphere leads to net emissions of 96 Gt C over the last millennium. The underlying primary emissions are 108 and 53 Gt C for the industrial and preindustrial period, respectively. We have quantified the feedback of CO_2 emissions on land carbon uptake to be high especially during the preindustrial era: Here, the biosphere-atmosphere coupling reduces the impact of ALCC by 48%. Together with ocean uptake, only 21% of the emissions remain airborne. This keeps the human impact on atmospheric CO_2 small over much of the preindustrial times, which is in agreement with estimates by Olofsson and Hickler [2008]; Strassmann et al. [2008]. However, by late medieval times atmospheric CO_2 rises above natural variability. Our study thus suggests that with respect to global CO_2 concentration, the "Anthropocene" began prior to the industrialization.

We also investigated the effects of rapid changes in ALCC as occurred in several regions over the last millennium due to epidemics and warfare. Indirect emissions from past ALCC can be overcome by carbon storage in regrowing vegetation only for events of long-lasting impact on population numbers. Only then regional carbon uptake occurs. The concurrent agricultural expansion in other regions, however, renders these events ineffective on the global scale. Such events thus cannot be the major cause for observed drops in global CO_2, as had been suggested by previous studies. It seems more likely that local climate has been altered due to the fast changes in biogeophysical fluxes [Pongratz et al., 2009].

This study applies an estimate of maximum ALCC to give an upper limit of possible human impact with respect to uncertainties in reconstructing land cover. Primary emissions are higher in this case, but the net effect on CO_2 and global mean temperature is little altered. The only forcing taken into account is the change in agricultural extent. Other types of ALCC such as deforestation for wood harvest are not included, but, as explained, are unlikely to have a major impact on our results. The long timescale further reduces the influence of uncertain parameters such as the decomposition rates of carbon released during ALCC. Largely unknown, however, are preindustrial land management practices in their impact on the carbon cycle. Low-tillage practices, for example, are known to reduce CO_2 fluxes from soils [e.g., Reicosky et al., 1997], but base data to follow changes in management techniques globally and through the last millennium does not exist. Since the largest emissions arise from vegetation carbon and since restorage occurs mainly on natural areas, we expect our results to be generally robust.

The present study is relevant beyond the historical perspective in several points. First, an analysis of sub-fluxes suggests that a large fraction of the land-use amplifier effect results from the indirect emissions and thus from past ALCC, rather than from the change in current turnover rates. Our analysis does not suggest that there is less importance of including this effect in estimates for future climate change, but it indicates that a second process acts next to the change in turnover rates. Being indirect emissions, this second process may either be reported as part of the primary ("book-keeping") emissions, or as part of the land-use amplifier effect, but must not be double-counted. It further is highly dependent on the assumptions made concerning the decay time of soil carbon on a decadal timescale. Model comparison and sensitivity studies should in the future aim at quantifying both processes separately with the associated uncertainty ranges.

Second, this study has found an anthropogenic influence on atmospheric CO_2 by late medieval times, and has indicated significant changes in the land and ocean carbon content even earlier. The carbon balance has already for this reason been out of equilibrium for many centuries. Furthermore, one third of the ALCC emissions until today have already been released by the end of the preindustrial era. This early disturbance of the carbon balance does not only imply a legacy of the past by increasing the atmospheric CO_2 concentration already prior to the industrialization. It also implies that the beginning of the simulation period usually applied for climate projections may be too late — our results indicate that climate-carbon cycle studies for present and future centuries, which usually start from an equilibrium state around 1850, start from a significantly disturbed state of the carbon cycle, possibly distorting model calibration against the industrial period.

Figure captions:

Fig. 1: Global land-atmosphere carbon fluxes, cumulative since AD 800. Positive values indicate release to the atmosphere. Thick lines are results for the best-guess ALCC reconstruction, thin lines for the high land cover dynamics. The shaded areas split up the best-guess primary emissions into direct (light) and indirect (dark) emissions. Simulations ctrl, L, LC as explained in Tab. 1. Values are 10-years running means.

Fig. 2: Accumulated changes since AD 800: (a) vegetation carbon pools, (b) soil carbon pools, (c) NEP. Thick lines are results for the best-guess ALCC reconstruction, thin lines for the high ALCC dynamics. Simulations ctrl, L, LC as explained in Tab. 1. Values are 30-years running means. Note that the curves of panels a and b add to the corresponding curves in Fig. 1 (with change of sign); L-ctrl in panel c refers to the indirect emissions in Fig. 1.

Fig. 3: Net emissions, coupling flux, and primary emissions of ALCC accumulated over the given time interval: preindustrial (AD 800–1850), industrial (AD 1850–2000), and future period (AD 2000–2100). Units are Gt C released from each grid cell. Simulations ctrl, L, LC as explained in Tab. 1.

Fig. 4: Changes in soil respiration R_h over changes in net primary productivity NPP for the indicated pairs of simulations. Gray shades indicate the time period: preindustrial (light), industrial (medium), future (dark). Simulations ctrl, L, LC as explained in Tab. 1. Values are 50-years running means.

Fig. 5: Change in the carbon stored globally on land, the ocean and sediment, and the atmosphere. Red lines are results for the best-guess ALCC reconstruction, blue lines for

the high ALCC dynamics. The yellow area indicates the 5–95 percentile of the control simulation. Values are 10-years running means.

Fig. 6: Change in the global mean surface temperature. Red lines are results for the best-guess ALCC reconstruction, blue lines for the high ALCC dynamics. The yellow area indicates the 5–95 percentile of the control simulation. Values are 30-years running means.

Fig. 7: Direct emissions (red) and indirect emissions from changes in NEP (blue) for China (top) and Europe (bottom). The gray boxes indicate the time periods of decreasing regional population. On the right axes in yellow, global total primary emissions are given. Values are 30-years running means.

Table 1. Description of model simulations.

acronym	target quantity	coupling	land cover maps	climate
ctrl	control simulation	full coupling	constant AD 800	control
LC	net emissions	full coupling	ALCC (*best-guess* and *high land cover dynamics*)	ALCC-driven
L	primary emissions ($ctrl - L$)	offline	ALCC (*best-guess* and *high land cover dynamics*)	control
	coupling flux ($L - LC$)			
C	loss of sink capacity ($(C - LC) - (ctrl - L)$)	offline	constant AD 800	ALCC-driven

Table 2. Biosphere-atmosphere carbon fluxes as described in the text, in Gt C accumulated over the respective time periods with 30-years running mean. Positive values indicate fluxes to atmosphere. NEP is net ecosystem productivity.

flux	time period			
	800–1850	1850–2000	2000–2100	800–2000
primary emissions	52.6	108.3	47.7	160.9
— direct emissions	30.4	63.7	21.5	94.1
— indirect emissions	22.2	44.6	26.2	66.8
coupling effect	-25.2	-39.6	-27.0	-64.8
— on NEP	-25.3	-41.4	-27.9	-66.7
— on direct emissions	-0.2	-1.8	-0.9	-2.0
net emissions	27.4	68.7	20.7	96.0
loss of sink capacity	0.3	4.0	4.3	4.3

Table 3. Primary emissions of this study in comparison to previous studies that include preindustrial estimates. Values are in Gt C and cumulative over the indicated time periods, with 30-years running mean for this study. Estimates of emissions prior to AD 800 in this study are estimated by assuming that the same amount of carbon is emitted per m^2 of agricultural expansion prior to AD 800 as averaged for AD 800 to 1850.

study	preindustrial	industrial	until present
DeFries et al. [1999]	48–57 (until 1850)	124 (1850–1990)	182–199 (until 1987)
Ruddiman [2003]	320 (4000 B.C.–1800)	–	–
Ruddiman [2007]	120–137 (–)	–	–
Strassmann et al. [2008]	45 (until 1700)	188 (1700–1999)	233 (until 1999)
Olofsson and Hickler [2008]	114 (4000 B.C.–1850)	148 (1850–1990)	262 (4000 B.C.–1990)
Olofsson and Hickler [2008] permanent ag. only	79 (4000 B.C.–1850)	115 (1850–1990)	194 (4000 B.C.–1990)
this study	53 (800–1850)	108 (1850–2000)	161 (800–2000)
this study	63 (until 1850)	108 (1850–2000)	171 (until 2000)

Table 4. Comparison of our results to previous studies: uptake of anthropogenic CO_2 emissions by land, atmosphere, and ocean including sediments. Values are in in Gt C and %, respectively, accumulated over the respective time periods with 30-years running mean. ALCC and fossil-fuel emissions are those considered in the studies. For Bolin et al. [2001]; Sabine et al. [2004], the mid-range values were adopted.

study	time period	emissions		uptake		
		ALCC	fossil fuel	land	ocean	atmosphere
Strassmann et al. [2008]	1700–1999	188	274	113 (24%)	156 (34%)	193 (42%)
House et al. [2002]	1800–2000	200	280	166 (34%)	124 (26%)	190 (40%)
Sabine et al. [2004]	1800–1994	140	244	101 (26%)	118 (31%)	165 (43%)
Bolin et al. [2001]	1850–1998	136	270	110 (27%)	120 (30%)	176 (43%)
Gitz and Ciais [2003]	1850–1998	139	269	110 (29%)	116 (30%)	157 (41%)
Houghton [2003b]	1980–1999	42	117	53 (33%)	41 (26%)	65 (41%)
this study	800–1850	53	0	25 (48%)	17 (31%)	11 (21%)
this study	1850–2000	108	0	40 (37%)	37 (34%)	31 (29%)
this study	2000–2100	48	0	27 (56%)	20 (41%)	1 (3%)

Acknowledgments. We thank Elke Stehfest for her help in extending the agricultural maps into the future, and Victor Brovkin and Katharina Six for helpful discussions. The simulations of this study were carried out as part of the "Community Simulations of the Last Millennium" (http://www.mpimet.mpg.de/en/wissenschaft/working-groups/millennium.html); we would like to thank all participants. We gratefully acknowledge Reiner Schnur for setting up and performing the simulations. These were carried out at the German Climate Computing Center (DKRZ). We further thank two anonymous reviewers for their helpful comments.

References

D. Archer, H. Kheshgi, and E. Maier-Reimer. Multiple timescales for neutralization of fossil fuel CO_2. *Geophys. Res. Lett.*, 24(4):405–408, 1997.

T. Barker, I. Bashmakov, A. Alharthi, M. Amann, L. Cifuentes, J. Drexhage, M. Duan, O. Edenhofer, B. Flannery, M. Grubb, M. Hoogwijk, F.I. Ibitoye, C.J. Jepma, W.A. Pizer, and K. Yamaji. Mitigation from a cross-sectoral perspective. In B. Metz, O.R. Davidson, P.R. Bosch, R. Dave, and L.A. Meyer, editors, *Climate Change 2007: Mitigation. Contribution of Working Group III to the Fourth Assessment Report of the Intergovernmental Panel on Climate Change*, pages 619–690. Cambridge University Press, Cambridge, United Kingdom and New York, NY, USA, 2007.

R.A. Betts. Biogeophysical impacts of land use on present-day climate: near-surface temperature change and radiative forcing. *Atmos. Sci. Lett.*, 1:doi:10.1006/asle.2001.0023, 2001.

B. Bolin, R. Sukumar, P. Ciais, W. Cramer, P. Jarvis, H. Kheshgi, C.A. Nobre, S. Semenov S, and W. Steffen. Global perspective. In R.T. Watson, I.R. Noble, B. Bolin, N.H. Ravindranath, D.J. Verardo, and D.J. Dokken, editors, *Land Use, Land-Use Change, and Forestry - A Special*

Report of the IPCC. Cambridge University Press, Cambridge, United Kingdom and New York, NY, USA, 2001.

G.B. Bonan, D. Pollard, and S.L. Thompson. Effects of boreal forest vegetation on global climate. *Nature*, 359:716–718, 1992.

L. Bounoua, R.S. DeFries, G.J. Collatz, P.J. Sellers, and H. Khan. Effects of land cover conversion on surface climate. *Climatic Change*, 52:29–64, 2002.

V. Brovkin, S. Sitch, W. von Bloh, M. Claussen, E. Bauer, and W. Cramer. Role of land cover changes for atmospheric CO_2 increase and climate change during the last 150 years. *Global Change Biol.*, 10:1253–1266, 2004.

V. Brovkin, M. Claussen, E. Driesschaert, T. Fichefet, D. Kicklighter, M.F. Loutre, H.D. Matthews, N. Ramankutty, M. Schaeffer, and A. Sokolov. Biogeophysical effects of historical land cover changes simulated by six Earth system models of intermediate complexity. *Clim. Dyn.*, 26:587–600, 2006.

M. Claussen, V. Brovkin, and A. Ganopolski. Biogeophysical versus biogeochemical feedbacks of large-scale land cover change. *Geophys. Res. Lett.*, 28(6):1011–1014, 2001.

M. Claussen, V. Brovkin, R. Calov, A. Ganopolski, and C. Kubatzki. Did humankind prevent a Holocene glaciation? *Climatic Change*, 69:409–417, 2005.

R.S. DeFries, C.B. Field, I. Fung, G.J. Collatz, and L. Bounoua. Combining satellite data and biogeochemical models to estimate global effects of human-induced land cover change on carbon emissions and primary productivity. *Global Biogeochem. Cycles*, 13(3):803–815, 1999.

R.S. DeFries, L. Bounoua, and G.J. Collatz. Human modification of the landscape and surface climate in the next fifty years. *Global Change Biol.*, 8:438–458, 2002.

K.L. Denman, G. Brasseur, A. Chidthaisong, P. Ciais, P.M. Cox, R.E. Dickinson, D. Hauglustaine, C. Heinze, E. Holland, D. Jacob, U. Lohmann, S. Ramachandran, P.L. da Silva Dias, S.C. Wofsy, and X. Zhang. Couplings Between Changes in the Climate System and Biogeochemistry. In S. Solomon, D. Qin, M. Manning, Z. Chen, M. Marquis, K.B. Averyt, M. Tignor, and H.L. Miller, editors, *Climate Change 2007: The Physical Science Basis. Contribution of Working Group I to the Fourth Assessment Report of the Intergovernmental Panel on Climate Change*. Cambridge University Press, Cambridge, United Kingdom and New York, NY, USA, 2007.

V. Gitz and P. Ciais. Amplifying effects of land-use change on future atmospheric CO_2 levels. *Global Biogeochem. Cycles*, 17(1):doi:10.1029/2002GB001963, 2003.

L.B. Guo and R.M. Gifford. Soil carbon stocks and land use change: a meta analysis. *Global Change Biol.*, 8:345–360, 2002.

R.A. Houghton. The annual net flux of carbon to the atmosphere from changes in land use 1850–1990. *Tellus*, 51(B):298–313, 1999.

R.A. Houghton. Revised estimates of the annual net flux of carbon to the atmosphere from changes in land use 1850–2000. *Tellus*, 55(B):378–390, 2003a.

R.A. Houghton. Why are estimates of the terrestrial carbon balance so different? *Global Change Biol.*, 9:500–509, 2003b.

R.A. Houghton and C.L. Goodale. Effects of land-use change on the carbon balance of terrestrial ecosystems. In R. Houghton R. DeFries, G. Asner, editor, *Ecosystems and Land Use Change*, volume 153, pages 85–98. Geophysical Monograph Series, 2004.

R.A. Houghton, J.E. Hobbie, J.M. Melillo, B. Moore, B.J. Peterson, G.R. Shaver, and G.M. Woodwell. Changes in the carbon content of terrestrial biota and soils between 1860 and 1980:

A net release of CO_2 to the atmosphere. *Ecol. Monogr.*, 53(3):235–262, 1983.

J.I. House, I.C. Prentice, and C. Le Quéré. Maximum impacts of future reforestation or deforestation on atmospheric CO_2. *Global Change Biol.*, 8:1047–1052, 2002.

A. Jain and X. Yang. Modeling the effects of two different land cover change data sets on the carbon stocks of plants and soils in concert with CO_2 and climate change. *Global Biogeochem. Cycles*, 19:GB2015, doi:10.1029/2004GB002349, 2005.

F. Joos, S. Gerber, I.C. Prentice, B.L. Otto-Bliesner, and P.J. Valdes. Transient simulations of Holocene atmospheric carbon dioxide and terrestrial carbon since the Last Glacial Maximum. *Global Biogeochem. Cycles*, 18:GB2002, 2004.

G. Marland, B. Andres, and T. Boden. *Global CO_2 emissions from fossil-fuel burning, cement manufacture, and gas flaring: 1751-2005.* Carbon Dioxide Information Analysis Center, 2008.

S.J. Marsland, H. Haak, J.H. Jungclaus, M. Latif, and F. Roeske. The Max-Planck-Institute global ocean/sea ice model with orthogonal curvilinear coordinates. *Ocean Modell*, 5:91–127, 2003.

C. McEvedy and R. Jones. *Atlas of World Population History.* Penguin Books, Harmondsworth, 1978.

A.D. McGuire, S. Sitch, J.S. Clein, R. Dargaville, G. Esser, J. Foley, M. Heimann, F. Joos, J. Kaplan, D.W. Kicklighter, R.A. Meier, J.M. Melillo, B. Moore II, I.C. Prentice, N. Ramankutty, T. Reichenau, A. Schloss, H. Tian, L.J. Williams, and U. Wittenberg. Carbon balance of the terrestrial biosphere in the twentieth century: Analyses of CO_2, climate and land use effects with four process-based ecosystem models. *Global Biogeochem. Cycles*, 15:183–206, 2001.

R. Moss, M. Babiker, S. Brinkman, E. Calvo, T. Carter, J. Edmonds, I. Elgizouli, S. Emori, L. Erda, K. Hibbard, R. Jones, M. Kainuma, J. Kelleher, J.F. Lamarque, M. Manning,

B. Matthews, J. Meehl, L. Meyer, J. Mitchell, N. Nakicenovic, B. O'Neill, R. Pichs, K. Riahi, S. Rose, P. Runci, R. Stouffer, D. van Vuuren, J. Weyant, T. Wilbanks, J.P. van Ypersele, and M. Zurek. *Towards New Scenarios for Analysis of Emissions, Climate Change, Impacts, and Response Strategies*. Intergovernmental Panel on Climate Change, Geneva, 2008.

D. Murty, M.U.F. Kirschbaum, R.E. McMurtrie, and H. McGilvray. Does conversion of forest to agricultural land change soil carbon and nitrogen? a review of the literature. *Global Change Biol.*, 8:105–123, 2002.

N. Nakicenovic, J. Alcamo, G. Davis, B. de Vries, J. Fenhann, S. Gaffin, K. Gregory, A. Grübler, T.Y. Jung, T. Kram, E.L. La Rovere, L. Michaelis, S. Mori, T. Morita, W. Pepper, H. Pitcher, L. Price, K. Riahi, A. Roehrl, H.-H. Rogner, A. Sankovski, M. Schlesinger, P. Shukla, S. Smith, R. Swart, S. van Rooijen, N. Victor, and Z. Dadi. Special Report on Emissions Scenarios. page http://www.ipcc.ch/ipccreports/sres/emission/index.html. Cambridge Univ. Press, Cambridge, 2000.

J. Olofsson and T. Hickler. Effects of human land-use on the global carbon cycle during the last 6,000 years. *Vegetation History and Archeobotany*, 17:605–615, 2008.

J. Pongratz, C. Reick, T. Raddatz, and M. Claussen. A reconstruction of global agricultural areas and land cover for the last millennium. *Global Biogeochem. Cycles*, 22(GB3018, doi:10.1029/2007GB003153), 2008.

J. Pongratz, T. Raddatz, C.H. Reick, M. Esch, and M. Claussen. Radiative forcing from anthropogenic land cover change since A.D. 800. *Geophys. Res. Lett.*, 36(L02709, doi:10.1029/2008GL036394), 2009.

T.J. Raddatz, C.H. Reick, W. Knorr, J. Kattge, E. Roeckner, R. Schnur, K.-G. Schnitzler, P. Wetzel, and J. Jungclaus. Will the tropical land biosphere dominate the climate-carbon cycle feedback during the twenty-first century? *Clim. Dyn.*, 29:565–574, 2007.

D.C. Reicosky, W.A. Dugas, and H.A. Torbert. Tillage-induced soil carbon dioxide loss from different cropping systems. *Soil and Tillage Research*, 41(1–2):105–118, 1997.

E. Roeckner, G. Bäuml, L. Bonaventura, R. Brokopf, M. Esch, M. Giorgetta, S. Hagemann, I. Kirchner, L. Kornblueh, E. Manzini, A. Rhodin, U. Schlese, U. Schulzweida, and A. Tompkins. *The atmospheric general circulation model ECHAM5. Part I: Model description*, volume 349. Report, Max Planck Institute for Meteorology, Hamburg, Germany, 2003.

W. Ruddiman. The anthropogenic greenhouse era began thousands of years ago. *Climatic Change*, 61:261–293, 2003.

W. Ruddiman. The early anthropogenic hypothesis: Challenges and responses. *Rev. Geophys.*, 45, RG 4001:37 pp., 2007.

C.L. Sabine, R.A. Feely, N. Gruber, R.M. Key, K. Lee, J.L. Bullister, R. Wanninkhof, C.S. Wong, D.W.R. Wallace, B. Tilbrook, F.J. Millero, T.-H. Peng, A. Kozyr, T. Ono, and A.F. Rios. The oceanic sink for anthropogenic CO_2. *Science*, 305:367–371, 2004.

D. Schimel, J.I. House, K.A. Hibbard, P. Bousquet, P. Ciais, P. Peylin, B.H. Braswell, M.J. Apps, D. Baker, A. Bondeau, J. Canadell, G. Churkina, W. Cramer, A.S. Denning, C.B. Field, P. Priedlingstein, C. Goodale, M. Heimann, R.A. Houghton, J.M. Melillo, B. Moore III, D. Murdiyarso, I. Noble, S.W. Pacala, I.C. Prentice, M.R. Raupach, P.J. Rayner, R.J. Scholes, W.L. Steffen, and C. Wirth. Recent patterns and mechanisms of carbon exchange by terrestrial ecosystems. *Nature*, 414:169–172, 2001.

S. Sitch, V. Brovkin, W. von Bloh, D. van Vuuren, B. Eickhout, and A. Ganopolski. Impacts of future land cover changes on atmospheric CO_2 and climate. *Global Biogeochem. Cycles*, 19 (GB2013, doi:10.1029/2004GB002311), 2005.

K.M. Strassmann, F. Joos, and G. Fischer. Simulating effects of land use changes on carbon fluxes: past contributions to atmospheric CO_2 increases and future commitments due to losses of terrestrial sink capacity. *Tellus*, 60B:583–603, 2008.

P. M. Vitousek, H. A. Mooney, J. Lubchenco, and J. M. Melillo. Human domination of earth's ecosystems. *Science*, 277(5325):494–499, 1997.

P. Wetzel, A. Winguth, and E. Maier-Reimer. Sea-to-air CO_2 fluxes from 1948 to 2003. *Global Biogeochem. Cycles*, 19(GB2005):doi:10.1029/2004GB002339, 2005.

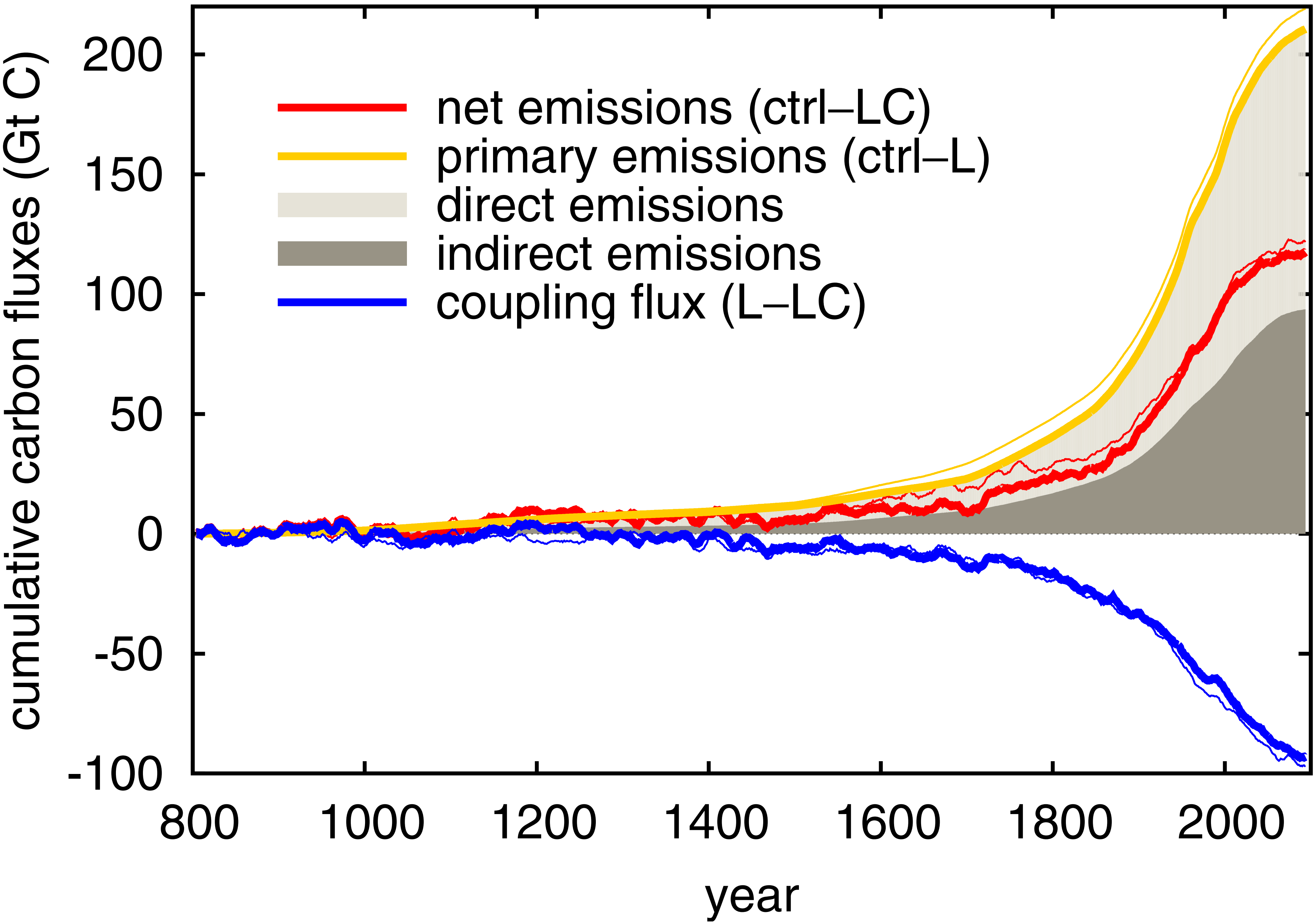

net emissions (ctrl–LC)
primary emissions (ctrl–L)
direct emissions
indirect emissions
coupling flux (L–LC)
cumulative carbon fluxes (Gt C)
200
150
100
50
0
-50
-100
800
1000
1200
1400
1600
1800
2000
year

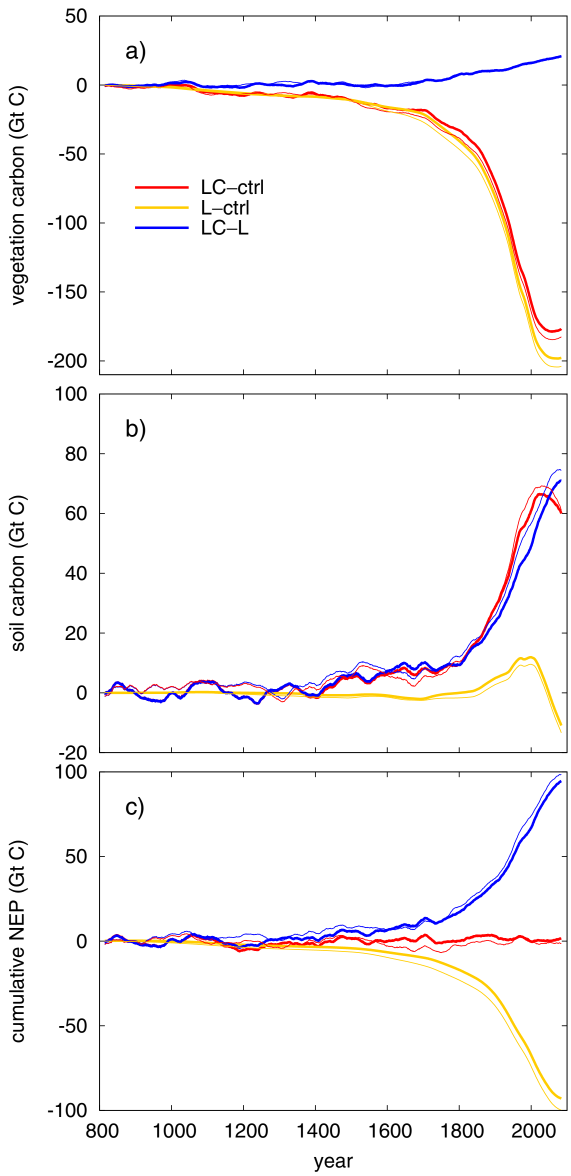

a)
b)
c)
LC−ctrl
L−ctrl
LC−L
vegetation carbon (Gt C)
soil carbon (Gt C)
cumulative NEP (Gt C)
50
0
-50
-100
-150
-200
100
80
60
40
20
0
-20
100
50
0
-50
-100
800
1000
1200
1400
1600
1800
2000
year

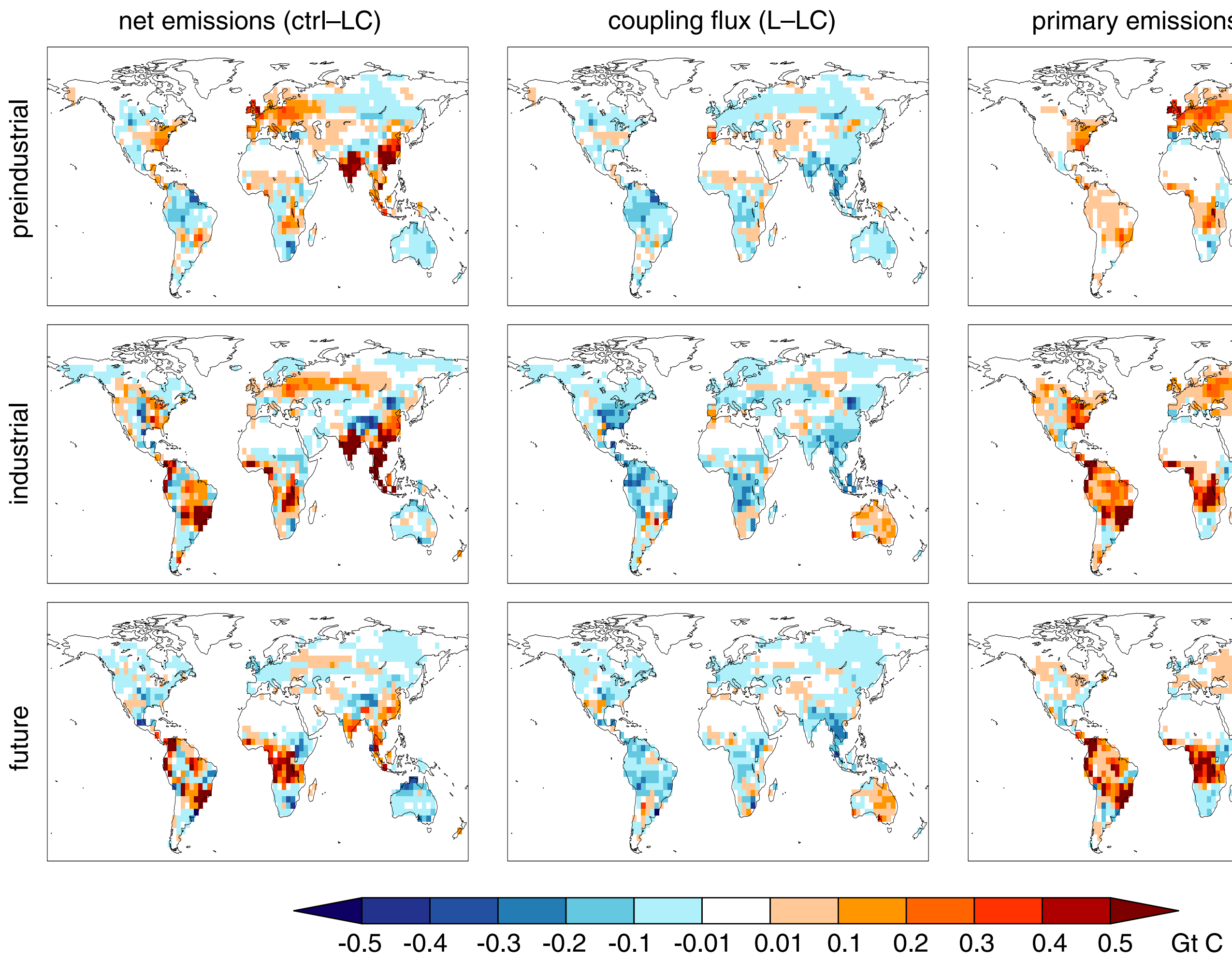
net emissions (ctrl–LC)
coupling flux (L–LC)
primary emissions (ctrl–L)
preindustrial
industrial
future
-0.5
-0.4
-0.3
-0.2
-0.1
-0.01
0.01
0.1
0.2
0.3
0.4
0.5
Gt C

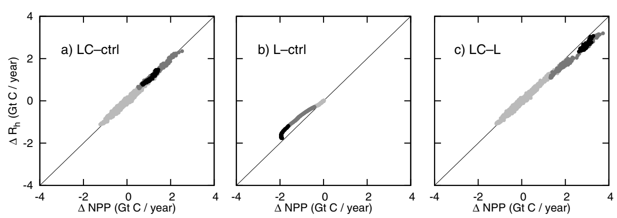

a) LC–ctrl
b) L–ctrl
c) LC–L
Δ R_h (Gt C / year)
Δ NPP (Gt C / year)
Δ NPP (Gt C / year)
Δ NPP (Gt C / year)
4
2
0
-2
-4
-4
-2
0
2
4

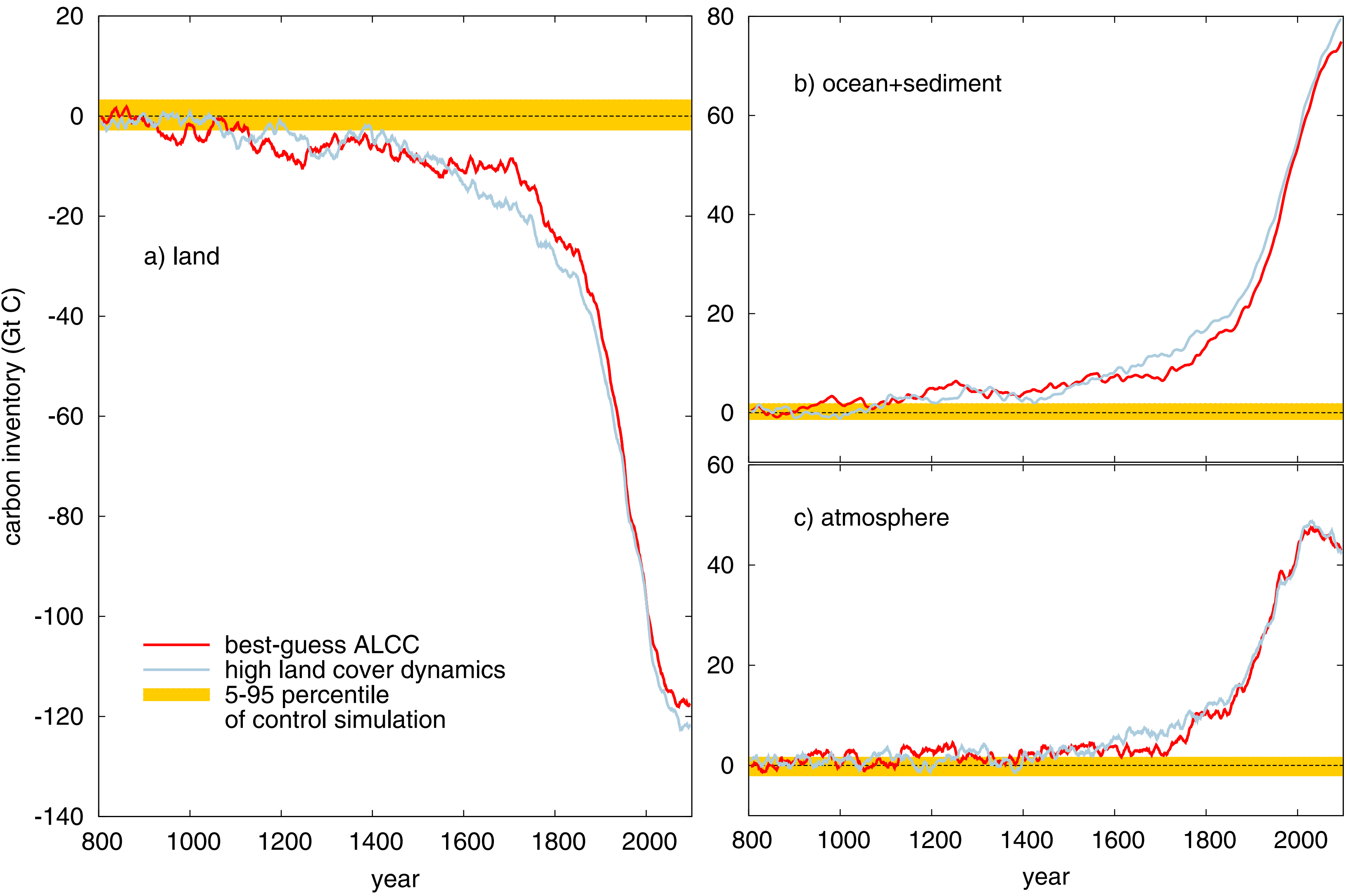

a) land
b) ocean+sediment
c) atmosphere
best-guess ALCC
high land cover dynamics
5-95 percentile
of control simulation
carbon inventory (Gt C)
year
20
0
-20
-40
-60
-80
-100
-120
-140
80
60
40
20
800
1000
1200
1400
1600
1800
2000

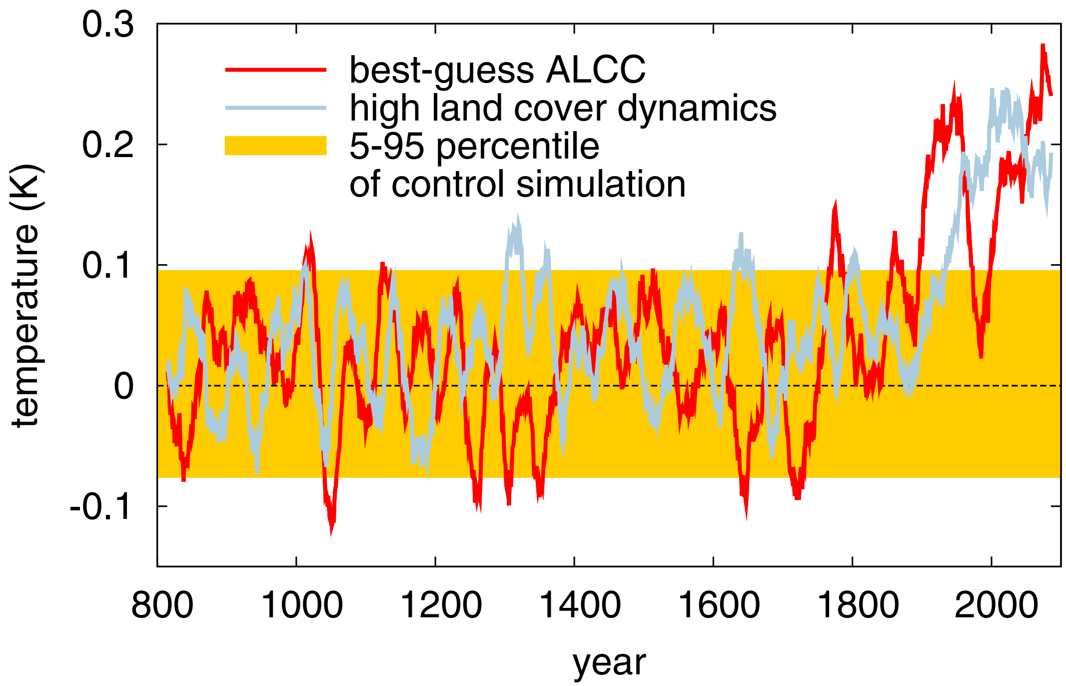
best-guess ALCC
high land cover dynamics
5-95 percentile
of control simulation
0.3
0.2
0.1
0
-0.1
temperature (K)
800
1000
1200
1400
1600
1800
2000
year

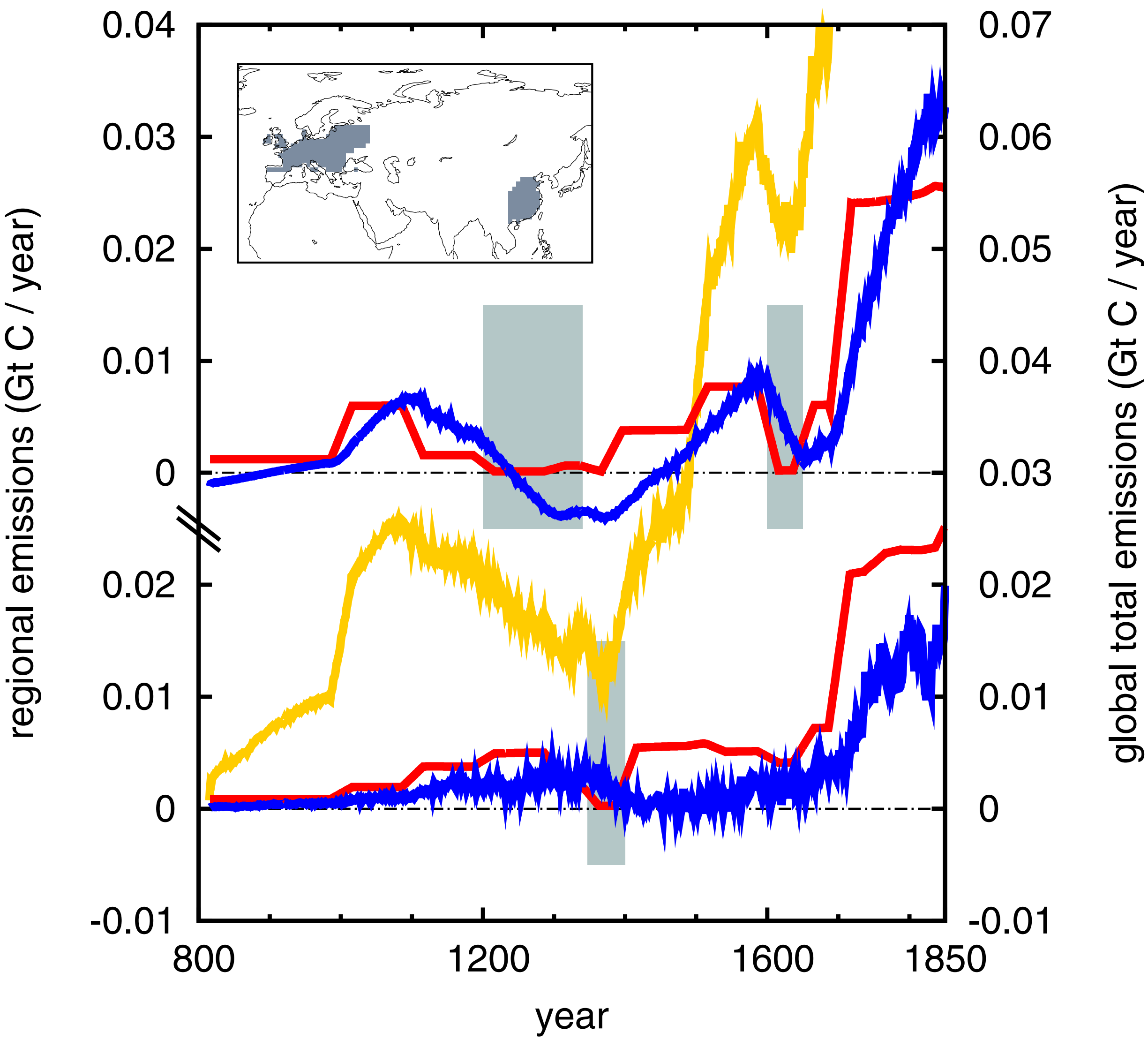

regional emissions (Gt C / year)
global total emissions (Gt C / year)
year
0.04
0.03
0.02
0.01
0
0.02
0.01
0
-0.01
0.07
0.06
0.05
0.04
0.03
0.02
0.01
0
-0.01
800
1200
1600
1850